18 Solitary Waves in Crustal Faults and their Application to Earthquakes

Victor G. Bykov

Institute of Tectonics and Geophysics, Far East Branch of the Russian Academy of Sciences, 65 Kim-Yu-Chen St., 680 000 Khabarovsk, Russia
e-mail: bykov@itig.as.khb.ru

18.1 Introduction

The problem related to crustal fault dynamics consists of identification of the processes and parameters that are responsible for sliding regimes in the faults. The concepts according to which the transition from creep to stick-slip along the crustal fault, in most cases accompanied by a tectonic earthquake, is caused by geometrical inhomogeneities of fault surfaces, a decrease of friction in some segments of the fault and by anomalies of the pore pressure, are considered to be conventional (Ben-Zion and Rice 1995). The deformational waves propagating along the faults and excited by elastic-rebound in the foci of the past earthquakes may also initiate seismic slips in crustal faults (Ulomov 1993).

The deformational waves detected from changes in the geophysical fields (Nikolaevskiy 1998) are accompanied by migration of seismic activity in a number of cases (Ulomov 1993). The existence of these waves is known to be confirmed in the course of experimental studies of slow deformation processes in the crust (Nevskiy 1994). A lot of direct and indirect evidences (Nikolaevskiy 1996) show that slow tectonic deformations are propagating as solitary waves – solitons. For this reason, theoretical studies (Garagash 1996, Nikolaevskiy 1996, Nikolaevskiy and Ramazanov 1986) aimed at developing mathematical models that lead to soliton-like solutions and, at the same time, reflect the main features of wave deformation process occurring in the crust are of topical interest.

In this chapter it is shown that local deformation effects at the mesoscopic level related to decrease of friction at the contacts of inhomogeneous fault surfaces may cause solitary waves of activation whose evolution leads to macroscopic processes as seismic slips in crustal faults. The model

suggested describes the dynamics of relative displacements of fault surfaces including retarding and accumulation of energy necessary to provide a stick-slip process. As it is well known, the stick-slip is a necessary element to provide seismic events inside the earthquake focus. Analysis is made of asperity and friction effects in the fault on the evolution of velocity of waves of activation and also the amplitude and frequency of periodical load on fault dynamics. A relative role of different processes in the initiation of seismic slip is investigated.

18.2 Observational Evidence

The concept of the deformational (tectonic) waves generated in the Earth is based on the results of the study of spatio-temporal density distribution and processes of crustal deformation. The results of observation of the oriented earthquake migration of direct and indirect in-situ measurements of deformational waves or of their indications are most comprehensively shown and analyzed by Mogi (1968), Nersesov et al. (1990), Barabanov et al. (1994), Kasahara (1979), and Nikolaevskiy (1998).

Quantitatively, the deformational wave processes are displayed in the rate of the earthquake foci migration and the presence of geophysical field anomalies close to the faults. In conventional approach, the most characteristic rates of these processes and the corresponding waves can be divided into two groups (two scales of manifestation): global tectonic waves and deformational waves generated in the faults.

The global tectonic waves with velocities of 10-100 km/year are observed in the following phenomena: the oriented migration of large earthquakes (Stein et al. 1997); seismic velocity anomalies (temporal variations of seismic wave velocities, travel-times and time discrepancies) (Nevskiy et al. 1987); changes of the underground water table along the fault zone due to waves (Barabanov et al. 1994); deformographic measurements (Ishii et al. 1979); cyclic migration of aseismic gaps in the Earth's mantle (Nikolaevskiy 1998); oscillation motions of seismic reflectors (Bazavluk and Yudakhin 1993, Bormotov and Bykov 1999). Movement of slow tectonic deformations occurs along the deep faults in a narrow "corridor" (~100 km) (Nevskiy et al. 1989).

Rapid migration of seismic activity occurring in vast areas prior to or after large earthquakes testifies indirectly about the existence of the deformational waves with velocities of 1-10 km/day generated in the faults (Hill et al. 1995, Barabanov et al. 1994). The seismic activity can be detected from the observable radon, electrokinetic and hydrogeodynamic

signals (Nikolaevskiy 1998), and exciting of the stress-and-strain waves at the explosion and vibration slips in initiation in the fault zone (Ruzhich et al. 1999). Geophysical signals have a shape of solitary waves and are propagating along the crustal faults (Nikolaevskiy 1998).

18.3 Mathematical Model of Deformation Process

The model includes two most important mechanisms providing interaction of the fault surfaces: friction, simulated by introduction of gouge viscosity in the fault, and geometrical inhomogeneities which are characterized by ratio of scales of asperity and sinusoidal parts of the internal fault surfaces, and external load. Thus, we now postulate the following equation:

$$\frac{\partial^2 U}{\partial \xi^2} - \frac{\partial^2 U}{\partial \tau^2} = \sin U + \alpha \frac{\partial U}{\partial \tau} + \gamma(\xi)\delta(\xi - L)\sin U + \sigma(\tau), \qquad (18.1)$$

where $U = 2\pi u/a$, $\xi = \pi x/ap$, $\tau = \pi\omega_0 t/p$, $p^2 = a^2 D/4mgh$, $\omega_0^2 = D/m$, $\alpha \approx a\mu/d\Delta\rho\sqrt{gh}$, $\gamma = H/L$, U is the displacement of blocks located periodically along the fault length; a is the distance between the block centers; D is the tangential contact stiffness; m is the mass of the block; h is the distance between the block centers of the adjacent block layers; g is the gravity acceleration; μ is the viscosity of the layer between the blocks; d is the diameter of the circular contact of the blocks; Δ is the layer thickness; ρ is the density of the block material; α and γ are the parameters of friction and inhomogeneity, respectively; H, L are the height of asperities and the distance between them normalized to ap/π; $\delta(\xi)$ is the Dirac delta-function and $\sigma(\tau)$ is the function which reflects the external load at the contact of the fault surfaces. Figure 18.1 shows schematic presentation of the fault surfaces.

The left-hand side of the generalized sine-Gordon equation (18.1) corresponds to the wave operator applied to the relative displacement of the fault surfaces. In the right-hand side of Eq. (18.1) the first term characterizes the "restoring" force, originating due to shear along the sinusoidal-homogeneous surfaces of the fault; the second one – the friction force, which is proportional to the velocity relative to displacement; the third term corresponds to corrections for inhomogeneities which are distributed at a distance apL/π; the fourth one describes the initiation external load on the fault.

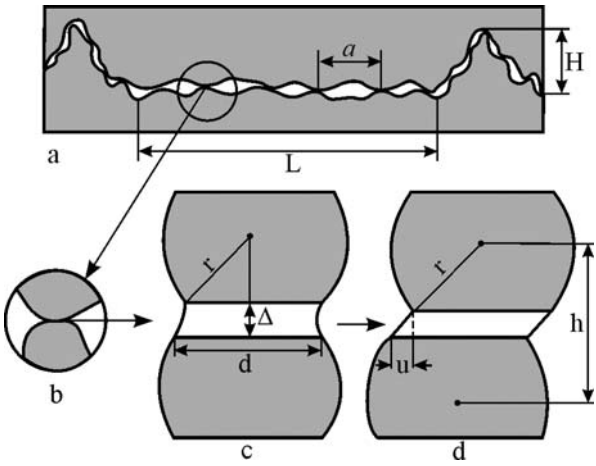

Fig. 18.1 Schematic diagram showing a change in contact between fault surfaces (a) and a change in the geometry of blocks contact (b-d): $a \approx 2r$, r is the radius of blocks

The expression for parameter α is obtained proceeding from the concepts of stick-slip (Dieterich 1987, Sleep 1995) and theory of dimension. Friction parameter α is mainly dependent on the average sizes of the blocks on the fault surface and also on the viscosity of the gouge, and assumes the values 0.01-1.0.

Inhomogeneity coefficient γ is equal to ratio of height H of the asperity to length L of the sector of the sinusoidal-inhomogeneous surface and characterizes regular point asperities of the relief of the fault surfaces. This element of the model reflects the fractal structure of the fault surfaces in the first approximation. Variation of the inhomogeneity coefficient γ is possible in the range from 0 to 1.0. The zero value means a complete absence of "cohesions" distinguished at the sinusoidal surface. The inhomogeneity coefficient value equal to 1.0 means coincidence of the height of the point asperity with the amplitude of the sinusoid.

Note that the effect of block rotation suggests an explanation for the sinusoidal character of the "restoring" forces (Nikolaevskiy 1996).

Integration of Eq. (18.1) has been made by the McLaughlin–Scott approximation method (Solerno et al. 1983), and numerical realization has been performed by the Runge-Kutta-Felberg scheme (Forsythe et al. 1977). The parameters of the medium were as follows: $\rho = 3\text{x}10^3$ kg/m^3, $D = 10^4$-10^6 N/m, $g = 9.8$ m/s^2, $r = 0.1$-1.0 m, $a = h = 2r$. Computation has been carried out with variation of the parameters of friction α and

inhomogeneity γ, which characterize the state of the contact at the fault, and also the value of $\sigma(\tau)$, that determines the external load.

18.4 Solitary Wave of Fault Activation

Profile of velocity v of the particles (Fig. 18.2) on the fault surfaces has a shape of the soliton $v(x,t) = v_{max}\mathrm{sech}(x–V_\alpha t)$, moving along the fault with a velocity V_α. Variation of friction parameter α in the sine-Gordon equation clears up significantly the reasons for variations of velocity V_α of the solitary wave in the crustal fault, as well as the consequences related to this variation. Value of velocity v of a particle on the fault surface is dependent on the state of the contact, that is, the value of the parameter α. It follows from the computations that in the case of low V_α, the value of v is insignificant and the stable sliding (creep) occurs. For the relatively high values of velocity V_α^{max} (of the order of 1-10 m/s) we obtain the soliton profile $v \sim 0.1$-1 m/s and the stepwise profile (kink) $u(x, t)$ (see Fig. 18.2). A similar relationship for dynamic characteristics but without time shift of the maxima of V_α and v can be obtained by analytical solution of the canonic sine-Gordon equation for a solitary wave in homogeneous fault without friction.

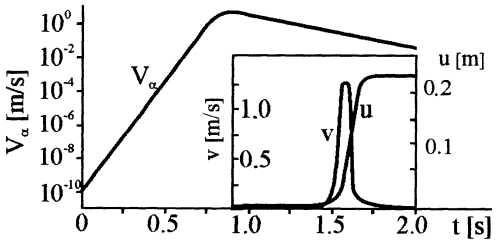

Fig. 18.2 Evolution of velocity V_α of wave of activation, displacement u and slip velocity v in the fault

Time interval between the peak values of V_α and v depends on the parameters α and γ. The moment of time when V_α attains the maximum value V_α^{max} always occurs earlier as compared to the calculated time of $v_{max.}$ Time lags between the transmitting of the solitary wave with the maximum velocity value and displacement u_{max} are stipulated by friction and inhomogeneities in the fault. The possibility of attaining high values of the relative slip gives grounds for calling the wave $v(V_\alpha)$ the solitary wave of

fault activation. The velocity maximum for the wave of activation, depending on the values of the chosen contact stiffness D in the faults does not exceed 10-100 m/s, that differs noticeably from velocities for the seismic waves, so from those for the deformational ones.

18.5 Evolution of Waves of Fault Activation

Velocity amplitude for the wave of activation increases to the value of about 0.9-1.8 m/s with subsequent transition to the stationary regime with the values $V_\alpha^{st} \approx 10^{-4}$-$10^{-2}$ m/s (Fig. 18.3), corresponding to the velocities of the deformational waves at inhomogeneity coefficient $\gamma = 0.1$-0.3 and a decrease of friction parameter α to 0.04. The creep regime is observed at $t = 11.0$-14.0 s. In the case of $\gamma > 0.3$, stability is acquired far later and V_α^{st} may have the values of the order of 10^{-6}-10^{-13} m/s. The value of V_α^{st} decreases with increase of γ, which is a result of the additional friction: the asperities make impediments at sliding more often, and retarding of the wave of activation is enhanced (the sliding is damped). Also, a transition of the system to the "fault is locked" regime is possible when $V_\alpha \to 0$.

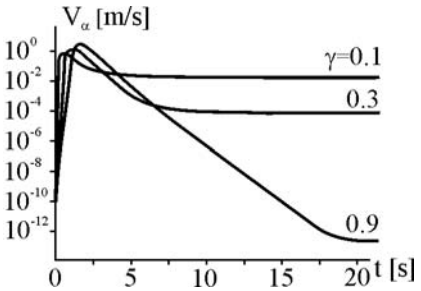

Fig. 18.3 Evolution of velocity V_α of wave of activation at different values of inhomogeneity coefficient γ and $\alpha = 0.04$

The greater the value of parameter γ ("cohesion" of the fault surfaces when other parameters are constant), the greater the velocity maximum of the wave of activation and the quicker the process of acquiring the stationary regime of activation. Thus, at the beginning of the stable sliding regime the inhomogeneities contribute to accumulation of greater elastic energy which is determined in dimensionless form by the component $(1+\gamma)\sin U$ in Eq. (18.1), and, vice versa, then they contribute to the fastest damping of the sliding. A long period of time is required to obtain V_α^{max} at an increase of α and decrease of γ.

Computation of fault dynamics shows that instability of sliding may be caused by a sharp decrease of the friction parameter which leads to an increase in the velocity of the wave of activation, and, consequently, in the slip velocity for the fault surfaces. Change in the sliding regimes dependent on the fault parameters occurs from 10 s ($\alpha = 0.04$, $\gamma = 0.1$) to 45 s ($\alpha = 0.01$, $\gamma = 0.1$).

18.6 Effect of Periodical Change of Friction in the Fault

Evolution of velocity V_α of the wave of activation in the fault depends on the friction parameter α. This parameter has a periodically changing component α_1 that corresponds to the regime of the cyclic perturbation contribution in some segments of the fault. Then the parameter α in Eq. (18.1) is transformed in $\alpha = \alpha_0 + \alpha_1 \sin(\tau/\eta)$, where α_0, α_1, η are some constants.

Results of computation of Eq. (18.1) at $\sigma(\tau) = 0$, $\eta = 10^2$, for varying α_0, α_1, and γ, show (see Fig. 18.4) that the maximum of velocity V_α is attained at t = 2-8 s from the perturbation moment, the time interval within which V_α corresponds to a slip 1-5 s. In fact, in real faults the sliding time is a value of the order of seconds at large earthquakes (Carlson 1991).

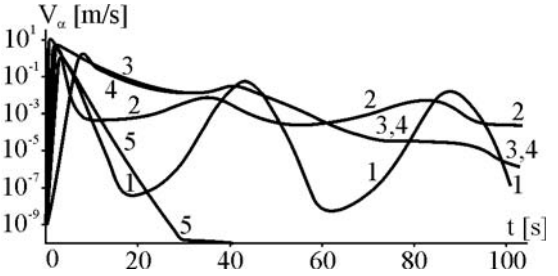

Fig. 18.4 Evolution of velocity V_α of wave of activation for different parameters of the state of contact for curves: (1) $\alpha_0 = 0.02$, $\alpha_1 = 0.09$, $\gamma = 0.9$; (2) $\alpha_0 = 0.09$, $\alpha_1 = 0.09$, $\gamma = 0.9$; (3) $\alpha_0 = 0.01$, $\alpha_1 = 0.01$, $\gamma = 0.9$; (4) $\alpha_0 = 0.01$, $\alpha_1 = 0.01$, $\gamma = 0.1$; (5) $\alpha_0 = 0.02$, $\alpha_1 = 0$, $\gamma = 0.9$

If the inhomogeneity parameter is constant, $\gamma = 0.9$, the maximum value of V_α is registered at the same time moment, but curves 1, 2 and 3 differ in amplitude: the minimum value of V_α corresponds to the maximum friction parameter α_0 (Fig. 18.4). Curves 3 and 4, computed at different γ and equal to α_0, α_1, at the time moment t = 30 s are merging and become indiscernible

further. It also follows from Fig. 18.4 that with increasing γ the maximum value of V_α is attained much earlier. At small α_0 and α_1 (curves 3 and 4) the velocity V_α is attenuating gradually to zero. At the higher values of α_0 and α_1 (curves 1 and 2), V_α acquires the periodical regime with velocities close to those of quick deformational waves reaching 1-10 km/day (Nikolaevskiy 1998). Evolution of V_α is represented by curve 5 without periodically changing additional friction ($\alpha_1 = 0$). This computation corresponds to a single generation of the solitary wave with transition of the system in the "fault is locked" regime.

Figure 18.4 shows that periodical generation of waves of activation with the velocities commensurable with those for the deformational waves is possible only under a certain state of the contacts of fault surfaces, that is, a combination of the friction and inhomogeneity parameters.

From this it follows that Eq. (18.1) can be applied for modelling of the seismic process at the appropriate choice of the corresponding parameters. Similar cyclic changes in the slip velocity and displacement in the fault zone were obtained due to periodical variations of stress (Dieterich 1987) and pore pressure (Sleep 1995) in the models of unstable sliding.

The increase in amplitude α_1 of the periodical friction component leads to a decrease in the maximum velocity value v of the seismic slip in the fault if other parameters of the model are constant. On the contrary, the increase of inhomogeneity parameter γ, which characterizes "cohesion" of the fault surfaces, causes the amplitude increase of velocity $v_{\max}$ of the seismic slip.

18.7 Effect of Periodical Change of External Load

Seismoactive faults undergo permanent external initiation effects of stress changes due to Earth tides, deformational waves from earthquakes or hydrological factors. Being active, these faults can generate oscillations, thus affecting other faults. Initiation of seismic slip may start because of inhomogeneity of physical properties along the faults due to constant external load.

We will simulate initiation of external load on the fault by including in Eq. (18.1) another periodical function $\sigma(\tau) = \sigma_0 \sin(\Omega\tau)$, where σ_0 and Ω are the dimensionless amplitude and frequency of the external load, the friction parameter α being constant. The instable slip being not affected by the external load, following (Sobolev et al. 1995), will be further called a

natural slip, while that initiated by the additional periodical external load – the initiated one.

The profile of velocity V_α of a solitary wave (curves 2 and 3) propagating along the fault differs sharply from the profile of velocity in the case with the natural slip (curve 1) (Fig. 18.5a). Within the initial part of velocity curves V_α the shape of the curves coincides for all the cases, but it has significant distinctions after the velocity maximum is attained. At higher frequencies (curve 3), V_α represents a periodical curve simulated by a descending part of the velocity curve V_α, which is computed in the absence of the source of external load (curve 1). The low-frequency ($\Omega = 0.1$) external load causes smoother changes of V_α, and the internal friction in the fault is not capable of compensating to the full extent the influence of the external load (Fig. 18.5a).

It follows from Fig. 18.5b that the first initiated slip occurs earlier at any frequency of the external load as compared to the natural one (curve 1). For this version of the computation, the time interval ΔT between $V_\alpha^{\max}$ and $v_{\max}$ is larger for the natural slip (curve 1) than for the initiated one (curves 2 and 3). This time, the interval increases with increasing frequency of the external load. The maximum velocity values of the wave of activation V_α, as well as those of slip velocity $v_{\max}$, correspond to the minimum frequency of the external sinusoidal load ($\Omega = 0.1$).

The time delay of the initiated dynamic slip decreases with increasing amplitude of the external load (Fig. 18.6). This agrees well with laboratory

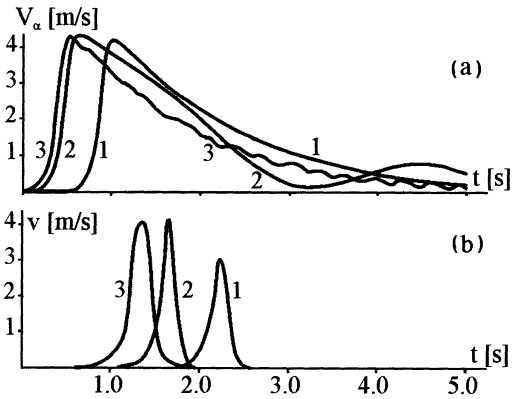

Fig. 18.5 Evolution of velocity of wave of activation V_α (a), and slip velocity v (b) at natural (1) and initiated (2, 3) slips. Parameters: $\alpha = 0.04$, $\gamma = 0.9$; $\sigma_0 = 0$ and $\Omega = 0$ for curve 1; $\sigma_0 = 0.01$ and $\Omega = 0.1$ for curve 2, $\sigma_0 = 0.01$ and $\Omega = 1.0$ for curve 3

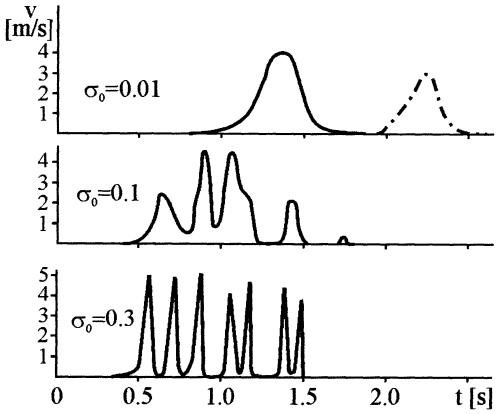

Fig. 18.6 Change of velocity of initiated slip v at constant frequency of external load $\Omega = 1.0$ and different amplitudes of load σ_0. The dot-dash line – natural slip velocity profile. Parameters: $\alpha = 0.04$, $\gamma = 0.9$

(Sobolev et al. 1991) and field (Ruzhich et al. 1999) experiments. A number of slips occur instead of one slippage, and the velocity amplitude of the first slip is the maximum one. The slip velocity amplitudes and the time intervals between them are not equal. The values of velocity maxima coincide for almost all these seismic slips. The slip velocities are weakly dependent on the amplitude σ_0 of the external load (Figs. 18.6 and 18.7). The number of slips is proportional to the amplitude of the load. The number of slips increases with an increase in the frequency of the constant sinusoidal load, while the time interval between the successive slips decreases (Fig. 18.6). This also coincides with the experiments (Ruzhich et al. 1999, Sobolev et al. 1995).

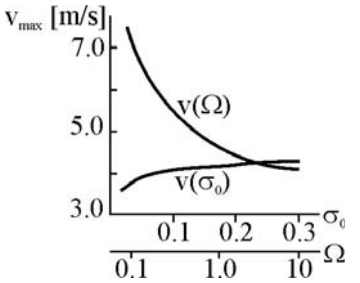

Fig. 18.7 Dependence of slip velocity maximum v_{max} in the fault on the frequency Ω ($\sigma_0 = 0.1$) and the amplitude σ_0 ($\Omega = 10$) of the external load. Parameters: $\alpha = 0.04$, $\gamma = 0.9$

A decrease in the frequency of the external load Ω leads to a significant amplitude increase in the slip velocity (Fig. 18.7). This is of particular importance if we take into consideration that the process is starting to be extremely sensitive to the external load at the final stage of earthquake preparation. Thus, we can consider the external load on the fault as an amplification of the wave of activation by the deformational waves with different frequency, radiated by an impact, explosion or earthquake.

It follows from the computed characteristics of the slips with different physical and mechanical parameters of the fault that the intensity and amplitude of the velocity of the initiated slip depend on the state of contacts of fault surfaces.

18.8 Conclusions

1. The generalized sine-Gordon equation can be applied for modeling peculiarities of fault dynamics. In fact, contribution of perturbation in the sine-Gordon equation in the form of friction and inhomogeneities leads to the solutions of the solitary-like waves that can be interpreted as the waves of fault activation.

2. The value of velocity for these waves regulates the sliding regime in the fault. The value of $v_{\max}$ of the wave of activation increases with increasing velocity V_α of the wave. The slip velocity increases sharply for the wave velocity V_α of 1 m/s and higher, and the values of displacement u are compatible with the displacements of the fault surfaces that are observed for earthquakes.

3. At definite values of friction and inhomogeneity parameters, α and γ, the solitary wave "acquires" the stationary regime with the values of $V_\alpha \sim 10^{-4}$-10^{-1} m/s or 10 km per day that correspond to the deformational waves. Earthquakes may be a source for deformational waves. These waves, migrating along the fault, may trigger the subsequent seismic events.

4. Periodical changes in the friction parameter in the generalized sine-Gordon equation (18.1), which models, for example, the weakening of the fault due to cyclic fluid flow, lead to a periodical generation of waves with the velocities characteristic of the observed deformational waves.

5. External periodical loading is the effective mechanism of the initiation of unstable dynamic slip. The external high-frequency load is probable to initiate the fault activation, but it does not provide periodical generation of the deformational waves and manifestation of seismic slips, as in the case with the cyclically changing friction inside the fault.

6. It is just the frequency of external loading that influences mainly the intensity of fault initiation, that is, the value of ν_{max} and the time interval between them. The amplitude increase of the sinusoidal external loading leads to a reduction in the time delay of the initiated stick-slip.

Acknowledgment. This research was supported by the Russian Basic Research Foundation (Grant 04-05-97001).

References

Barabanov VL, Grinevskiy AO, Belikov VM, Ishankuliev GA (1994) Migration of the crustal earthquakes. In: Nikolaev AV (ed) Dynamic processes in the geophysical medium. Nauka, Moscow, pp 149-167 (in Russian)

Bazavluk TA, Yudakhin FN (1993) Deformation waves in earth crust of Tien-Shan on seismological data. Dokl Akad Nauk **329**: 565-570 (in Russian)

Ben-Zion Y, Rice JR (1995) Slip patterns and earthquake populations along different classes of faults in elastic solids. J Geophys Res **100**: 12,959-12,983

Bormotov VA, Bykov VG (1999) Seismological monitoring of the deformation process. Geol Pacific Ocean **18**: 17-25

Carlson JM (1991) Time intervals between characteristic earthquakes and correlations with smaller events: An analysis based on a mechanical model of a fault. J Geophys Res **96**: 4255-4267

Dieterich JH (1987) Nucleation and triggering of earthquake slip: effect of periodic stresses. Tectonophysics **144**: 127-139

Forsythe GE, Malcolm MA, Moler CB (1977) Computer methods for mathematical computations. Prentice Hall, Englewood Cliffs, New York

Garagash IA (1996) Microdeformation of the prestress discrete geophysical media. Dokl Akad Nauk **347**: 95-98 (in Russian)

Hill DP, Johnston MJS, Langbein JO, Bilham R (1995) Response of Long Valley caldera to the M_w = 7.3 Landers, California, earthquake. J Geophys Res **100**: 12,985-13,005

Ishii H, Takagi A, Suzuki S (1979) Characteristic movement of crustal deformation in Northeast Honshu, Japan. Gerlands Beitr Geophys **88**: 163-169

Kasahara K (1979) Migration of crustal deformation. Tectonophysics **53**: 329-341

Mogi K (1968) Migration of seismic activity. Bull Earth Res Inst Tokyo Univ **46**: 53-74

Nersesov IL, Lukk AA, Zhuravlev VI, Galaganov ON (1990) On propagation of strain waves in the crust of South Middle Asia. Fizika Zemli **5**: 102-112 (in Russian)

Nevskiy MV (1994) Extra long period waves of deformations on the lithosphere plate boundaries. In: Nikolaev AV (ed) Dynamic processes in the geophysical medium. Nauka, Moscow, pp 40-55 (in Russian)

Nevskiy MV, Morozova LA, Zhurba MN (1987) The effect of propagation of the long-period strain perturbations. Dokl Akad Nauk **296**: 1090-1093 (in Russian)

Nevskiy MV, Morozova LA, Fuis GS (1989) Long-period strain waves. In: Sadovskiy MA (ed) Discrete properties of the geophysical medium. Nauka, Moscow, pp 18-33 (in Russian)

Nikolaevskiy VN (1996) Geomechanics and Fluidodynamics: with Applications to Reservoir Engineering. Kluwer Acad Publish, Dordrecht Boston London

Nikolaevskiy VN (1998) Tectonic stress migration as nonlinear wave process along earth crust faults. In: Adachi T, Oka F, Yashima A (eds) Proc of the Fourth Intern. Workshop on Localization and Bifurcation Theory for Soils and Rocks, Gifu, Japan, 28 Sept. - 2 Oct. 1997. AA Balkema, Rotterdam, pp 137-142

Nikolaevskiy VN, Ramazanov TK (1986) Generation and propagation of tectonic waves along deep faults. Fizika Zemli **10**: 3-13 (in Russian)

Ruzhich VV, Truskov VA, Chernykh EN, Smekalin OP (1999) Recent movements in the fault zones of Pribaikalia and mechanisms of their initiation. Geo Geofiz **40**: 360-372 (in Russian)

Sleep N (1995) Ductile creep, compaction, and rate and state dependent friction within major fault zones. J Geophys Res **100**: 13,065-13,080

Sobolev GA, Koltsov AV, Andreev VO (1991) Effect of oscillation triggering in modelling of earthquake. Dokl Akad Nauk SSSR **319**: 337-341(in Russian)

Sobolev GA, Ponomarev AV, Koltsov AV (1995) Excitation of vibrations in a model of seismic source. Fizika Zemli **12**: 72-78 (in Russian)

Solerno M, Soerensen MP, Skovgaard O, Christiansen PL (1983) Perturbation theories for sine – Gordone soliton dynamics. Wave Motion **5**: 49-58

Stein RS, Barka AA, Dieterich JH (1997) Progressive failure on the North Anatolian fault since 1939 by earthquake stress triggering. Geophys J Int **128**: 594-604

Ulomov VI (1993) Seismogeodynamic activization waves and the long-term prediction of earthquakes. Fizika Zemli **4**: 43-53 (in Russian)